Single-Walled Carbon Nanotubes Deliver Peptide Antigen into Dendritic Cells and Enhance IgG Responses to Tumor-Associated Antigens

Carlos H. Villa,[†] Tao Dao,[†] Ian Ahearn,[⊥] Nicole Fehrenbacher,[⊥] Emily Casey,[†] Diego A. Rey,[‡] Tatyana Korontsvit,[†] Victoriya Zakhaleva,[†] Carl A. Batt,[§] Mark R. Philips,[⊥] and David A. Scheinberg[†,*]

[†]Molecular Pharmacology and Chemistry and Program. Departments of Medicine and Radiology, Memorial Sloan Kettering Cancer Center, New York, New York 10021, United States, Departments of [‡]Biomedical Engineering and [§]Food Science, Cornell University, Ithaca, New York 14853, United States, and [⊥]Departments of Medicine, Cell Biology, and Pharmacology, New York University School of Medicine, New York, New York 10016, United States

ABSTRACT We studied the feasibility of using single-wall carbon nanotubes (SWNTs) as antigen carriers to improve immune responses to peptides that are weak immunogens, a characteristic typical of human tumor antigens. Binding and presentation of peptide antigens by the MHC molecules of antigen presenting cells (APCs) is essential to mounting an effective immune response. The Wilm's tumor protein (WT1) is upregulated in many human leukemias and cancers and several vaccines directed at this protein are in human clinical trials. WT1 peptide 427 induces human CD4 T cell responses in the context of multiple human HLA-DR.B1 molecules, but the peptide has a poor binding affinity to BALB/c mouse MHC class II molecules. We used novel, spectrally quantifiable chemical approaches to covalently append large numbers of peptide ligands (0.4 mmol/g) onto solubilized SWNT scaffolds. Peptide-SWNT constructs were rapidly internalized into professional APCs (dendritic cells and macrophages) within minutes *in vitro*, in a dose dependent manner. Immunization of BALB/c mice with the SWNT—peptide constructs mixed with immunological adjuvant induced specific IgG responses against the peptide, while the peptide alone or peptide mixed with the adjuvant did not induce such a response. The conjugation of the peptide to SWNT did not enhance the peptide-specific CD4 T cell response in human and mouse cells, *in vitro*. The solubilized SWNTs alone were nontoxic *in vitro*, and we did not detect antibody responses to SWNT *in vivo*. These results demonstrated that SWNTs are able to serve as antigen carriers for delivery into APCs to induce humoral immune responses against weak tumor antigens.

KEYWORDS: carbon nanotubes · nanomedicine · Wilms' tumor antigen · peptide vaccines · dendritic cells

Active specific immunotherapies (vaccines) take advantage of the ability of the immune system to recognize and react with foreign antigens. In the case of cancer vaccines, the antigens typically are not foreign, but overexpressed self-antigens on the surface or inside the tumor cell, some of which are then presented on the cell surface in the context of HLA molecules for recognition by T-cells.[1,2] The generation of an immune response generally requires peptide presentation by dendritic cells (DCs), which are the most effective antigen presenting cells (APCs).[3,4] Tumor self-antigens are generally poorly immunogenic and the host bearing the tumor either does not recognize the antigen or is tolerant to it.[5,6] While a number of strategies have been used to enhance the immunogenicity of tumor peptide antigens and break the self-tolerance, soluble peptides are poor immunogens, and effective immunization strategies require delivery formulations that include carrier molecules or adjuvants. Great advances have been made within the past decade in the discovery of new adjuvants suitable for clinical use, including cytokines,[7] saponins, CpG motifs,[8] and heat shock proteins[9] that can stimulate the innate immune system and induce strong adaptive immune responses. However, their biological activities are normally short-lived, requiring several doses to be administered. Materials made from synthetic and natural sources such as dendrimers or keyhole limpet hemocyanin (KLH), have been proposed as potential carrier molecules.[10,11] The potent immunogenicity and lack of flexibility of these carrier molecules can lead to the problem of carrier-induced suppression. The host immune system becomes overwhelmed with the maintenance of a polyclonal response to the carrier molecule, thereby limiting the ability to generate a focused response to the antigen of choice, which is detrimental to the efficacy of the vaccine.[12] Thus, there is a need for new carriers, especially those that efficiently deliver the antigens into professional APCs, such as DCs.

A promising approach to improve the immunogenicity of proteins and peptides for cancer vaccines is the use of particulate

* Address correspondence to d-scheinberg@ski.mskcc.org.

Received for review January 17, 2011 and accepted June 18, 2011.

Published online June 19, 2011
10.1021/nn200182x

vaccines.[13] Conjugation of antigenic epitopes to particulate scaffolds has shown that the particles improve immune responses and that the response is most improved when the particles are on the nanoscale.[14] This discovery has introduced the concept of nanovaccines, where changes in the nanoscale architecture of particulate vaccine materials can direct the characteristics of the immune response.[15] An important characteristic of nanovaccines is their enhancement of delivery to APCs. Antigen delivery through nanoparticles also alters cellular trafficking and can serve as an intracellular depot of antigen, both of which improve the immune response to the delivered antigen. However, most studies of nanoparticulate vaccines have used the strongly immunogenic, egg protein, OVA as the model antigen in initial investigations; peptides derived from this foreign protein are already known to be highly immunogenic.

As a nanomaterial of unique physical and chemical properties, carbon nanotubes have attracted considerable interest in biomedical applications,[16] including their use as nanovaccine scaffolds. Because of their propensity to internalize into a wide variety of cell types and through several mechanisms,[17−19] they appear to be particularly suited to deliver antigenic epitopes to APCs. In addition, carbon nanotubes have a unique geometry (very high aspect ratio) that may inherently alter the immunogenicity of appended antigens. Single-walled carbon nanotubes (SWNTs) also have a large available surface area for chemical modification, with every atom inherently at the nanotube surface. Furthermore, well-functionalized, dispersed carbon nanotubes do not appear to have inherent toxicity[20] (in contrast to unmodified carbon nanotubes[21]), and can bear large numbers of peptide ligands. There is also evidence that carbon nanotubes can produce immune responses when covalently linked to highly immunogenic peptide sequences.[22] However, there are no reports on the use of carbon nanotubes (CNTs) to deliver antigen to primary human DCs, nor the demonstration of improvement of immunogenicity of therapeutically relevant antigens administered with common adjuvants. Furthermore, there is continuing debate about the inherent immunogenicity of SWNTs and their ability to augment immune responses.[23]

In the current study, we aimed to demonstrate that carbon nanotube−peptide constructs could improve the immunogenicity of a weakly immunogenic, clinically relevant cancer-associated peptide. Wilm's tumor antigen (WT1) is widely used in human trials as a cancer vaccine.[24−26] A 19 amino acid peptide named WT1-Pep427 derived from WT1 protein was chosen for study because the peptide has high binding affinity across multiple human HLA-DR haplotypes and induces strong CD4 T cell responses in humans, but is a poor binder to both I-Ed and I-Ad class II molecules of BALB/c mice. We used spectrally quantifiable chemical approaches to covalently append large numbers of peptide ligands onto solubilized SWNT scaffolds. The SWNTs were covalently modified on their sidewalls with hydrophilic ethylene glycol using 1,3-dipolar cycloaddition of azomethine ylides. We then investigated the kinetics and cellular pharmacology of the nanotube interaction with APCs *in vitro*; finally we asked whether these nanotube−peptide conjugates could improve immune responses *in vivo* in mice. We also demonstrated that the nanotube scaffold itself is noncytotoxic to human dendritic cells and is nonimmunogenic.

RESULTS

Synthesis and Characterization of SWNT−4FB. The synthetic scheme for the nanotube−peptide conjugates used in this study is shown (Figure 1). SWNTs covalently functionalized with primary amines (SWNT−NH_2) were produced as described previously.[27] In previous studies[28] we characterized the physical properties of identically prepared SWNT−NH_2 material and the chromatographic methods used to prepare it. This synthetic scheme reproducibly produces functionalized SWNTs in the size range of 50−400 nm. The SWNT−NH_2 material was a dark brown solid whose amine content was 0.4−0.6 mmol/g, as quantified through the Kaiser ninhydrin assay and in agreement with previous syntheses. The purity was >90%, as verified by reverse phase HPLC (Figure 1b). The solid SWNT−NH_2 was analyzed using Raman spectroscopy which demonstrated that the nanotubes were highly functionalized, evidenced by a rise in the disorder band at ∼1360 cm^{-1}, as well as the major tangential mode peak at ∼1580 cm^{-1}, characteristic of CNTs. The broadening of these peaks along with a broad increase in background signal also confirmed that the SWNTs were highly dispersed. The SWNT−NH_2 was then reacted with succinimidyl-4-formyl-benzoate, and the resulting aldehyde functionalized nanotubes (SWNT−4FB) were analyzed by reverse phase HPLC (Figure 2b) that demonstrated the high purity (>90%) of the material as well as similar retention time to the starting SWNT−NH_2. The conversion to aldehyde groups was also evident in the reduction of available amines to less than 0.05 mmol/g as measured by the Kaiser ninhydrin assay. The SWNT−4FB solid was also analyzed by transmission electron microscopy (TEM) (Figure 2c) to roughly determine nanotube lengths and found aggregates of nanotubes in the range on 50−400 nm, with high variability in nanotube length. This finding was in good correlation with sizes calculated from dynamic light scattering measurements on similarly functionalized SWNTs.[28] We also observed that individualized side-wall functionalized SWNTs had poor contrast on TEMs, likely due to reduced electron density upon covalent modification, making it difficult to observe individual tubes.

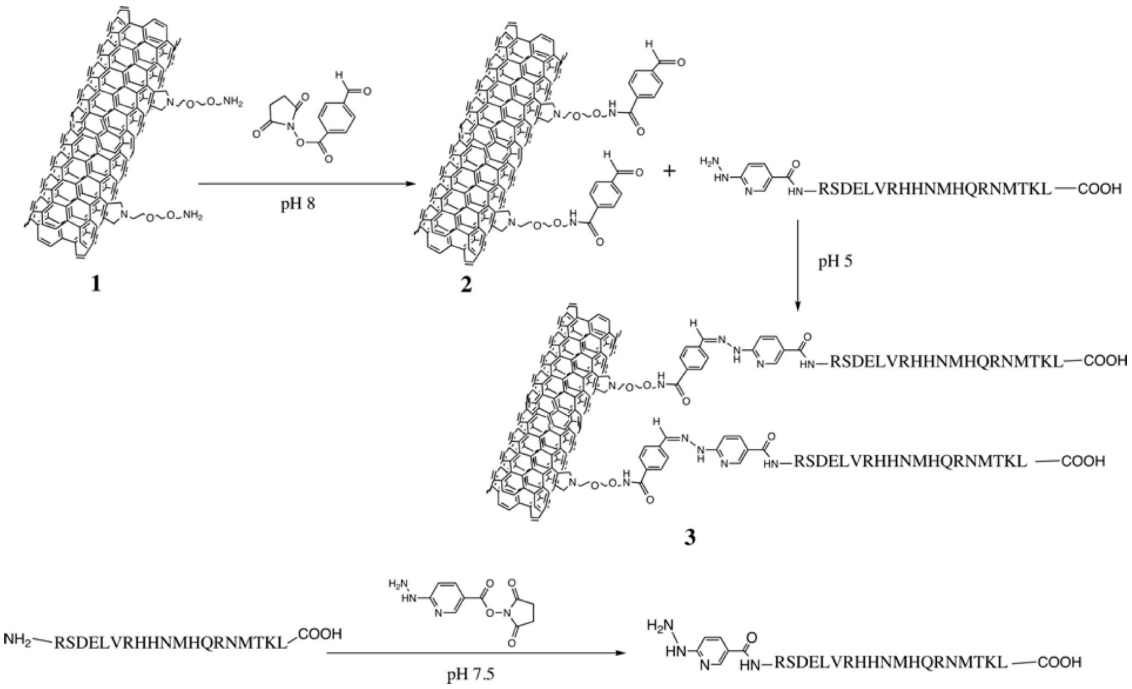

Figure 1. Synthetic scheme for the production of SWNT−peptide conjugates and modification of WT1Pep-427 with aromatic hydrazine groups.

Modification of WT1Pep427. A WT1 epitope bearing peptide (WT1Pep427, sequence: NH_2-RSDELVRHHN-MHQRNMTKL-COOH) was chosen based on previous studies that demonstrated that the peptide contains sequences capable of binding to MHC class II proteins (see above). The peptide was reacted with succinimidyl hydrazino nicotinamide at mildly basic pH (Figure 1) to introduce aromatic hydrazines at the amino terminus of the peptide, while avoiding modification of the lysine side chains (pK_a >10). The purity of the modified hydrazine modified peptide was >95% as determined by C18 reverse phase HPLC. The presence of hydrazine in the peptide was quantified through reaction with 2-sulfobenzaldehyde to form a quantifiable chromophore of λ_{max} = 350 nm. The remaining primary amine on the lysine side chain was quantified through a Kaiser ninhydrin assay. These analyses found a 1:1 ratio of hydrazine to amine, suggesting monomolecular modification at the amine terminus, with preservation of amines on lysine side chains.

Conjugation of SWNT−4FB with WT1Pep427-HyNic. The SWNT−4FB and WT1Pep427-HyNic were conjugated by reaction at mildly acidic pH. The addition of 20% acetonitrile to the reaction mixture helped to reduce aggregation of the nanotubes that had been observed in similar concentrated aqueous reactions. The SWNT−WT1Pep427 conjugate was purified from free WT1Pep427−HyNic by use of a C18 reverse-phase cartridge and analyzed by UV−vis spectroscopy. The absorbance spectrum demonstrated features of the expected SWNT spectrum, as well as a rise in absorbance at 354 nm attributable to the formation of the bis-aryl hydrazone linkage between the peptide and nanotube (Figure 2a). This difference in absorbance was quantifiable by subtraction of the spectrum of SWNT−NH_2. This calculation resulted in a peptide loading of 0.4−0.5 mmol of peptide per gram of SWNT, in line with the initial loading of primary amine groups. This loading represents roughly 50−75 peptides per 100 nm of nanotube length based on typical molecular weights of SWNTs. The purity of the material was confirmed by HPLC (Figure 2b), which also demonstrated that the bis-aryl hydrazone bonds were associated with the SWNTs based on the spectrum of the major peak and retention time similar to SWNTs starting material. HPLC also confirmed that the SWNT−WT1Pep427 conjugates did not contain free peptide, which would have eluted in the first 10 min of the solvent gradient.

Uptake of SWNT into Human Dendritic Cells. Peripheral blood mononuclear cells were isolated from normal human donors and cultured in the presence of GM-CSF and IL-4 to induce differentiation into immature dendritic cells. SWNT−4FB solid was dissolved in DMSO and then diluted into PBS. The SWNT−4FB solution in PBS was then added to immature DCs (day 5) at a range of concentrations from 0 to 100 μg/mL. The amount of DMSO in the final incubation conditions was always <0.15%. Control DCs were treated with identical volumes and concentrations of DMSO/PBS. Because the functionalized SWNTs possess inherent fluorescence across a range of excitation/emission wavelengths,[29] uptake could be monitored using flow cytometry, and signal from the SWNTs can be seen as an increase in fluorescence in any of the typical channels (FL2 and FL3

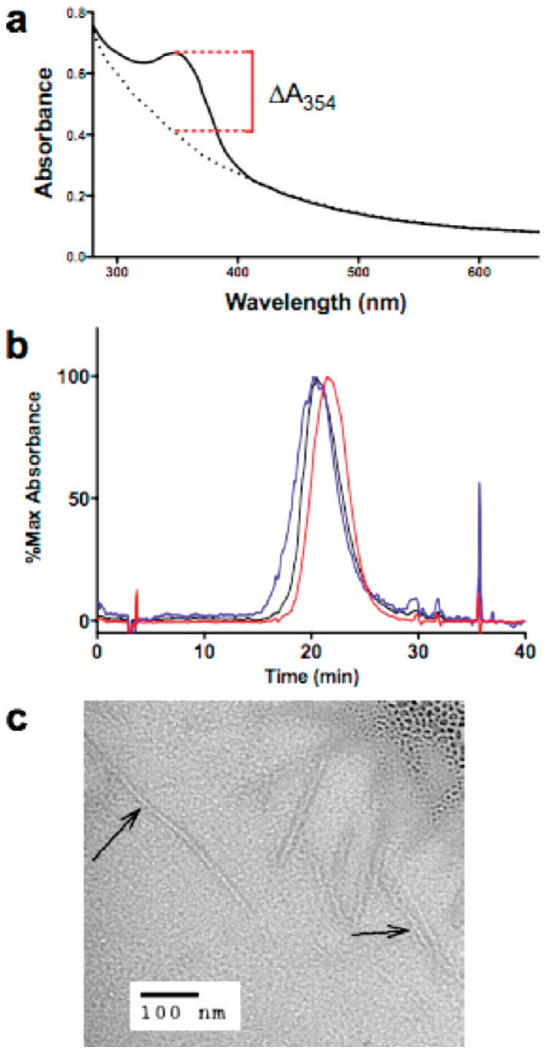

Figure 2. Characterization of functionalized SWNTs. (a) UV–vis spectrum of SWNT–WT1Pep427 (solid line) demonstrates a rise in absorbance at ~354 nm over the SWNT–4FB spectrum (dashed line). This peak is characteristic of the bis-aryl hydrazone bond formed between the modified peptide and the SWNT–4FB. (b) Reverse phase HPLC of the starting material SWNT–NH_2 (black), the SWNT–4FB intermediate (red), and the SWNT–WT1Pep427 conjugate (blue) demonstrate the purity of the three constructs. All peaks overlaid, and the spectrum of the major peak of SWNT–WT1Pep427 was consistent with the spectrum of the SWNT–WT1Pep427 shown above in panel a. (c) TEM of the SWNT–4FB used in these studies shows a polydisperse mixture with features characteristic of nanotubes.

are shown), or an increase in side-scattering intensity (due to light scattered by the internalized SWNTs). There was a dose-dependent increase in both cell-associated side-scatter and fluorescence in all channels (Figure 3a–c). Furthermore, uptake as measured by the shift in median fluorescence continued to increase at the highest dose (Figure 3d). There was no change in the forward-scattering intensity, suggesting no significant change in the cellular size.

To further define the uptake kinetics, mechanism, and cellular trafficking pattern of nanotube constructs, immature dendritic cells (day 5) were incubated with fluorescently labeled SWNTs at 1–10 μg/mL. Cells were then observed live, in real-time, using a temperature controlled confocal microscope imaging system. The characteristic morphology of the dendritic cells was evident. (Figure 4a.) We observed that uptake into the dendritic cells was immediate (within 5 min), and had a punctate pattern. Initial uptake on the periphery of the DCs appeared vesicular (Figure 4a–c, white arrows), and occurred within the first 15 min of addition of the SWNT constructs. After 15 min, the fluorescently labeled nanotubes accumulated in a diffuse perinuclear compartment (Figure 4a–c, arrowheads). This pattern of uptake was the same for either amine (SWNT–NH_2–AF555, Figure 4a) or aldehyde (SWNT–4FB–AF568, Figure 4b)-functionalized SWNTs. The kinetics and pattern of cellular trafficking was verified by using two differently labeled SWNTs. Cells were first treated with a red-labeled SWNT (SWNT–4FB–AF568) construct for 30 min, washed, then treated with a green-labeled SWNT contruct (SWNT–NH_2–AF488) and immediately imaged. The resulting image of this treament (Figure 4c) shows the early peripheral uptake in the green vesicles (Figure 4c-arrow) as well as the late accumulation of SWNTs in the red-stained perinucelar compartment (Figure 4c-arrowhead). This pattern of trafficking was also seen in similarly treated macrophages (Figure 4d).

The perinuclear compartment in the immature DCs was also relatively acidic, as it stained diffusely with a green lysosomal marker (Lysotracker green), and colocalized with the perinuclear uptake of red-labeled SWNT–4FB–AF568 constructs (Figure 4e). Lysosomes in immature dendritic cells are known to be sites rich in intracellular MHC class II molecules.[33] Interestingly, the cellular fate of internalized SWNTs was different in a Ras transformed fibroblast cell line (NIH-3T3, Figure 4f), where internalized SWNTs did not colocalize with lysosomal compartments or accumulate in a perinuclear compartment.

The rapid, robust, and vesicular uptake is consistent with macropinocytosis, known to be an important mechanism of macromolecular antigen uptake in immature dendritic cells.[30,31] Macropinocytosis in DCs is also known to concentrate macromolecules in intracellular vesicles and to traffic antigens to MHC class II rich compartments, desirable for antigen delivery. Phagocytosis, such as through mannose receptors, contributes additional capacity for antigen capture in DCs and may also contribute to SWNT uptake. Macropinocytosis in growth factor stimulated epithelial cells does not necessarily result in delivery to late endosomes or lysosomes,[32] likely explaining why the SWNTs did not colocalize with lysosomal markers in the Ras transformed fibroblasts.

To differentiate between receptor-independent and receptor-dependent (clathrin mediated) pinocytotic uptake mechanisms, DCs were treated with

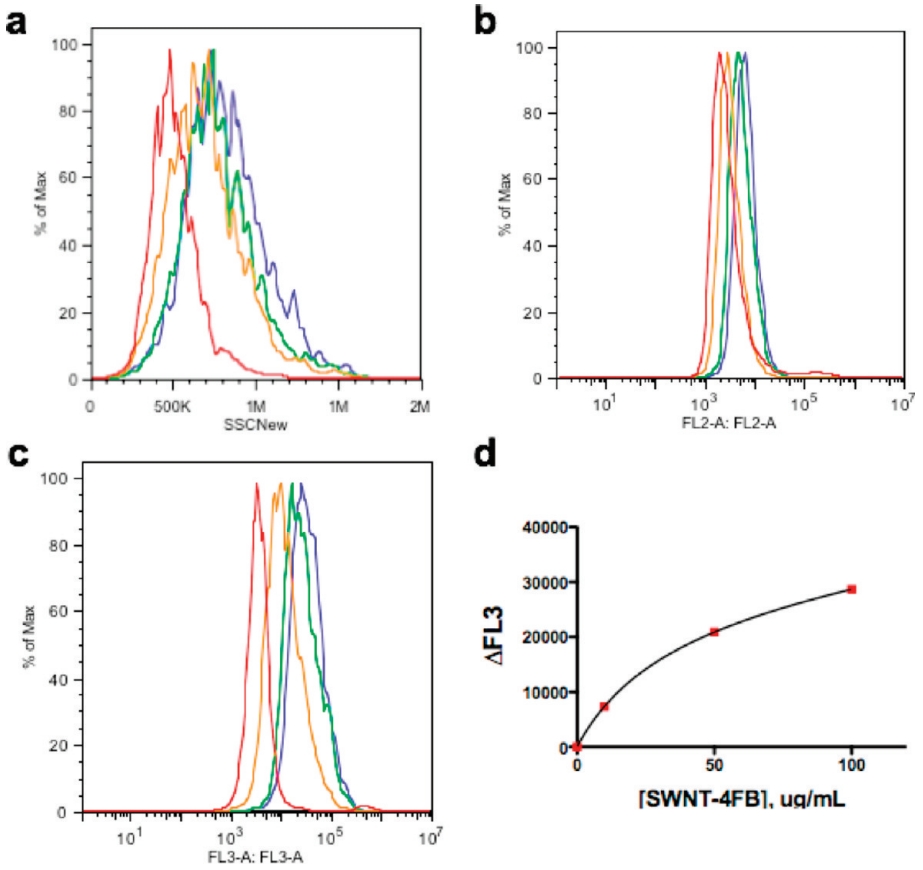

Figure 3. Internalization could be observed through (a) an increase in side-scatter intensity with increasing doses (0, red; 10, orange; 50, green; and 100 μg/mL, blue) and an increase in fluorescence intensity due to the broad intrinsic fluorescence of the SWNT−4FB. Fluorescence in channel (b) FL2 and (c) FL3 are shown. (d) The increase in fluorescence could be quantified as the shift in median fluorescence.

fluorescently labeled transferrin, a marker for clathrin-mediated endocytosis, along with labeled SWNT constructs. There was minimal colocalization with Tf around the periphery of the dendritic cells (Figure 4g), but some colocalization was seen in late accumulation in a perinuclear compartment (Figure 4h). This finding suggests that receptor-mediated (clathrin dependent) endocytosis is a relatively minor contributor to the uptake of SWNTs by antigen presenting cells. Receptor-mediated endocytosis in DCs can share the same ultimate fate as receptor-independent processes, which explains the late intracellular colocalization of SWNTs with Tf. While other mechanisms of uptake, such as direct membrane permeation, for SWNTs have been described,[17] it appears that in antigen presenting DCs, these pathways are minor contributors in comparison to the rapidity of macropinocytotic accumulation.

These findings suggest that in antigen presenting cells, SWNT constructs are trafficked to a degradative perinuclear region, likely through macropinocytosis, resulting in accumulation in a lysosomal perinuclear compartment. Phagocytosis may also contribute to internalization into DCs. These MHC class II-rich compartments are known sites of peptide processing, such as cleavage by cathepsins, for subsequent loading into MHC II proteins for presentation on the cell surface upon maturation of the DCs.[33,34] To confirm that peptide can be delivered to this compartment when covalently attached to SWNTs, dendritic cells were similarly treated with SWNT−WT1Pep427(FITC) conjugates in which the peptide was labeled with a fluorescein moiety on its lysine side chain. The nanotube was directly labeled with a near-infrared fluorophore (HiLyte Fluor 647). After treatment with the conjugate for 2.5 h, the cells were washed, fixed with neutral buffered formalin, stained with DAPI, and observed under a confocal microscope. A maximum intensity projection of a 10 μm thick section through a representative DC (Figure 4i) demonstrates that the peptide (green) and SWNT (red) colocalize to produce yellow staining in peripheral vesicles and a perinuclear compartment in similar fashion to that previously observed with live cells. The staining closest to the nucleus (Figure 4i, arrowhead) was stronger in the red channel (the SWNT) than the green (the peptide), suggesting cleavage of the peptide from the SWNT in the late vesicles. These microscopy analyses suggest that SWNT−peptide constructs are concentrated in intracellular vesicles in DCs, potentially enhancing peptide delivery into APCs.

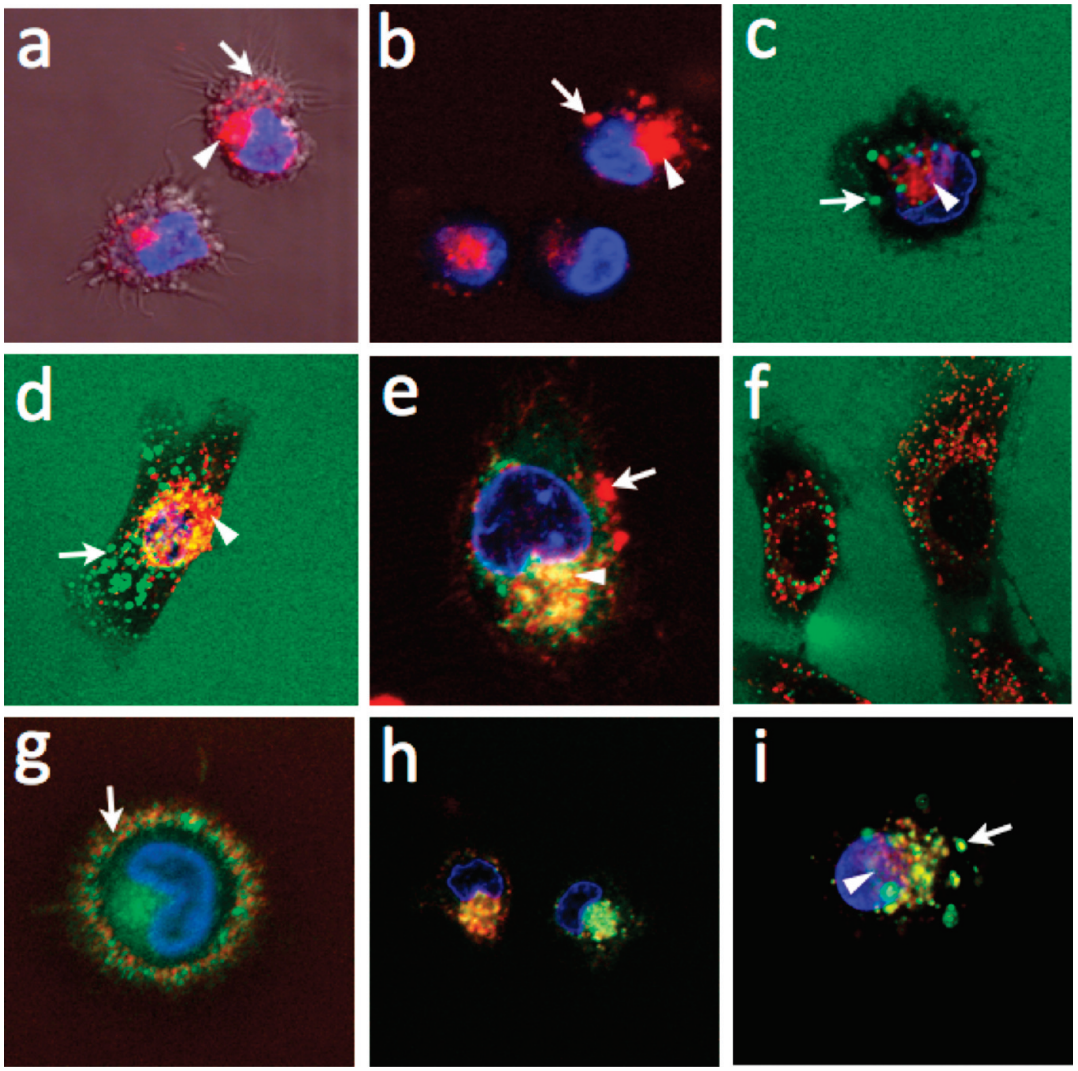

Figure 4. Tracking the internalization of SWNT constructs into DCs by confocal microscopy. Internalization followed a pattern of early peripheral vesicular uptake (white arrows), with transport to a perinuclear region (white arrowheads). Nuclei were counterstained with Hoechst (a–h) or DAPI (i). Cells were imaged live after 30 min incubation unless otherwise noted. Live DCs were treated with either (a) SWNT–NH_2–AF555 (red), or (b) SWNT–4FB–AF568 (red). No difference in uptake pattern was seen between the aldehyde and amine functionalized SWNTs. To track early and late uptake, DCs were treated with (c) SWNT–4FB–AF568 (red) for 30 min, washed, treated with SWNT–NH_2–AF488 (green), and immediately imaged. Similarly, macrophages were treated with (d) SWNT–4FB–AF568 (red) for 30 min, washed, treated with SWNT–NH_2–AF488 (green), and immediately imaged. For counterstaining studies, DCs were treated with (e) SWNT–4FB–AF568, washed after 30 min, and stained with Lysotracker (green), or NIH-3T3 fibroblast cells were treated with (f) SWNT–AF488–NH_2 (green) and Lysotracker (red). To track clathrin-mediated endocytosis, DCs were treated with both (g) SWNT–AF488–NH_2 (green) and Texas red labeled Transferrin (red) and immediately imaged, or DCs were treated with both (h) SWNT–AF488–NH_2 (green) and Texas red labeled Transferrin for 30 min, washed, and imaged thereafter. To track the uptake of SWNT–peptide into DCs, the SWNT was labeled with hiLyte Fluor 647 (red) and the attached peptide was labeled with fluorescein (green). DCs were then treated with SWNT–WT1Pep427(FITC) conjugate for 2.5 h, washed, fixed, stained with DAPI, and observed under a confocal microscope. A maximum intensity projection of a 10 μm thick section through a representative DC can be seen in panel i. Costaining in endocytic vesicles can be seen as the punctate yellow structures (arrow), while later perinuclear uptake appears stronger in the red channel (arrowhead).

Cytotoxicity of SWNT Constructs. Although robust uptake of SWNTs into DCs is favorable for the delivery of antigen into the cells, it was also important to demonstrate that the SWNTs themselves did not affect immature DC viability so that their antigen processing and presenting function is preserved. To measure any potential cytotoxic effect of SWNTs, immature (day 5) DCs were treated with varying concentrations of the SWNT–4FB scaffold up to 100 μg/mL. Cellular viability was assessed through an alamar blue assay for cellular metabolic activity, an ATP lite assay for cellular ATP production, and a bisbenzimide stain for cellular apoptosis (Figure 5). Treatment with SWNT–4FB up to 100 μg/mL did not demonstrate any dose-dependent cytotoxicity in any of the three assays. Cells were treated for up to 48 h without cytotoxic effects, a time scale long enough for internalization, processing, and presentation of antigen to immune effectors. At 48 h, the

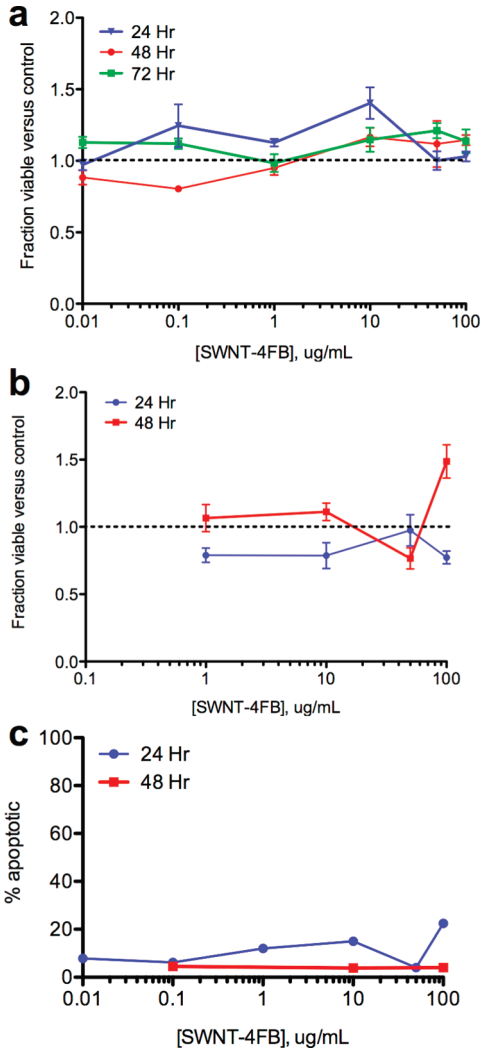

Figure 5. Cytotoxicity assay of SWNT–4FB in immature dendritic cells. No dose dependent cytotoxicity was observed up to 100 μg/mL (at 24, 48, and 72 h of treatment with SWNTs) when assayed by (a) alamar blue assay, (b) ATP lyte assay, or (c) bisbenzimide apoptosis assay.

dark color of the SWNT constructs was visible inside the immature DC when directly observed under light microscopy. The prolonged retention of SWNTs in viable DCs also suggests that the internalized SWNT–WT1Pep427 particles could serve as an intracellular reservoir of antigenic peptides. Overall, the results suggested that dendritic cells could internalize a large amount of SWNTs without compromising cellular integrity.

SWNT–peptide Generation of Human CD4 T Cell Response *in Vitro*. Having shown that SWNTs could be internalized by immature DCs without affecting cellular viability, it was important to demonstrate that internalized SWNT–peptide conjugates could induce peptide-specific immune responses. WT1-derived peptide WT1Pep427 (WT1Pep427) was identified in human studies as a valid CD4 T cell epitope with strong binding affinities to multiple HLA-DR.B1 molecules.[24] The peptide was shown to induce strong CD4 T cell responses in humans across a broad range of HLA-DR.B1 haplotypes. To test the impact of the SWNT conjugation on CD4 T cell response *in vitro*, we compared WT1Pep427 peptide alone with the peptide/SWNT conjugates in CD4 T cell stimulation and IFN-γ secretion. The WT1Pep427 peptide alone induced a strong CD4 T cell response, as shown previously.[24–26] Conjugating a peptide to a SWNT maintained, but did not enhance, the CD4 T cell response *in vitro* (Figure 6A). This suggests that once the T cell receptor (TCR) signaling reached a sustained level for its activation, increasing the density of the peptide/MHC complex (pMHC), mediated by SWNT delivery, was no longer required. This is an intrinsic property of T cell activation, as T cells need to recognize and respond to cognate pMHC ligands only at low density on the APC surface. On the other hand, although we expect the peptide to be cleaved from SWNTs in APCs, this process may have not been complete and thus may have affected the MHC binding and the presentation by APCs to T cells, resulting in a reduction of the CD4 T cell response. Importantly, stimulating CD4 T cells with SWNTs alone did not generate any responses against either the SWNTs or the peptide, indicating that the SWNTs are not immunogenic.

One possible explanation for the above experiments was that the stimulus was presented throughout the duration of culture and therefore, CD4 T cells may have been constantly exposed to a large amount of peptide stimulation. Therefore, we next tested if SWNT could enhance the CD4 T cell response in a setting of a shorter stimulation through kinetic enhancement of peptide delivery. For this purpose, autologous APCs were pulsed with the peptide, SWNT, or the peptide/SWNT construct for 6 h, 1 h, or 15 min, and the cells were washed extensively before coculturing with CD4 T cells. In all the time points, peptide specific responses could be produced. However, conjugation of peptide to SWNT again did not produce further enhancement of the CD4 T cell IFN-γ secretion. Figures 6B and 6C show representative data from 1 h and 15 min stimulations, respectively. These results suggested that the TCR stimulation of the WT1Pep427 peptide quickly reached saturation in the given durations and stimulation dosages, and conjugation to SWNT therefore maintained but did not further enhance the antigenic stimulation *in vitro* in human cells. Because SWNT–peptide conjugates were able to induce CD4 responses to known immunogenic antigens in human cells *in vitro* we therefore wanted to address the question of the SWNT–peptide conjugates' ablility to enhance the immune response in mice, both *in vitro* and *in vivo*, where WT1Pep427 in known to be a weakly immunogenic antigen.

Peptide/SWNT Construct Induces a Peptide-Specific IgG Response *in Vivo*. We next tested the hypothesis that the SWNT conjugation would enhance the delivery of a weak antigenic peptide and help elicit peptide-specific

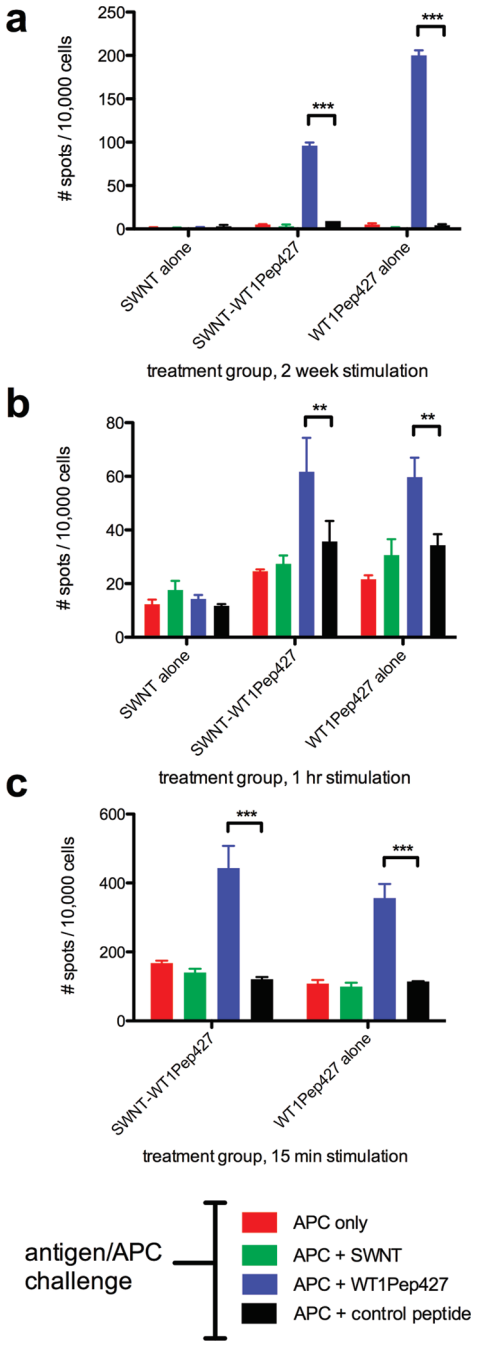

Figure 6. Generation of IFN-γ CD4 responses *in vitro* in human cells. IFN-γ ELISPOT by CD4 T cells stimulated with SWNT, WT1-Pep427, or WT1Pep427/SWNT constructs. CD4 T cells from a healthy donor were stimulated twice with APCs that were pulsed with SWNTs, WT1Pep427, or WT1Pep427/SWNT for the entire culturing time (a), 1 h (b), or 15 min (c) as described in the Methods section. Stimulated T cells were challenged in IFN-γ ELISPOT assay with the SWNT, WT1Pep427 peptide, or the irrelevant control peptide. The results represent the mean spots in triplicate cultures $\pm$SD. The figures show one representative data set from multiple similar experiments. Experiments included PHA as a positive control, not shown. Statistical analyses were performed using two-way ANOVA with Bonferroni post-test ($p < 0.01$, ***$p < .001$).**

immune responses *in vivo*. Although WT1Pep427 has a strong affinity for human HLA-DR.B1 molecules, the peptide has a poor binding affinity to both I-Ed and I-Ad MHC class II molecules of BALB/c mice, and thus would be an ideal model peptide to address the question in these mice. The binding scores of the peptide to I-Ed and for I-Ad molecules are as low as 17.8 and −0.65, respectively, by RANKPEP prediction (http://bio.dfci.harvard.edu/Tools/rankpep.html). We hypothesized that the conjugation of multiple peptides onto a single scaffold would allow the antigens to be taken up and presented at a higher density to overcome the activation threshold of mouse CD4 T cells. Furthermore, nanoparticulate SWNT−WT1Pep427 conjugates may alter trafficking and clearance both intracellularly and at the tissue level *in vivo*, such as providing a depot effect. This could potentially, in turn, enhance the induction of a peptide-specific IgG response.

CD4 T cell stimulation experiments similar to those performed with human donor cells were performed with lymphocytes isolated from the spleens of BALB/c mice. Cells were stimulated with peptide alone, peptide-SWNT conjugates, and SWNTs alone. No peptide specific response was detected in an IFN-γ ELISPOT assay of mouse CD4 cells *in vitro* (see Supporting Information), confirming the relatively weak immunogenicity of WT1Pep427 in mouse immune cells. For vaccination studies *in vivo,* BALB/c mice were immunized with five different constructs: SWNT alone, WT1-Pep427 peptide alone, WT1Pep427 conjugated to SWNT (WT1Pep427/SWNT), WT1Pep427 mixed with adjuvant Titer Max, or the WT1Pep427/SWNT mixed with Titer Max. After three and four immunizations, the peptide-specific serum IgG responses were evaluated by ELISA assay. Among the five immunization groups, only the mice injected with peptide/SWNT construct mixed with TiterMax induced significant IgG responses specific for WT1Pep427 peptide (Figure 7A,B). This antibody response was reproducibly observed in repeated trials in different cohorts of mice. In all experiments, no IgG response appeared to be directed against the SWNTs, although the amount of SWNTs on the plates could not be quantified. The mice immunized with SWNTs, WT1Pep427 alone, WT1Pep427/SWNT, or the WT1Pep427 mixed with TiterMax did not show detectable IgG responses. No IgM response was observed in any of the groups either (see Supporting Information), suggesting there was adequate CD4 T cell help in SWNT−WT1Pep427 treated mice to promote antibody class switch. Three immunizations also induced the specific IgG response to WT1Pep427 peptide, but to a lesser degree than four immunizations, confirming that repetitive immunizations were required for boosting the antibody response.

DISCUSSION

In the present study we demonstrated successful conjugation of large numbers of MHC class II peptide ligands onto solubilized SWNT scaffolds. The nanotube

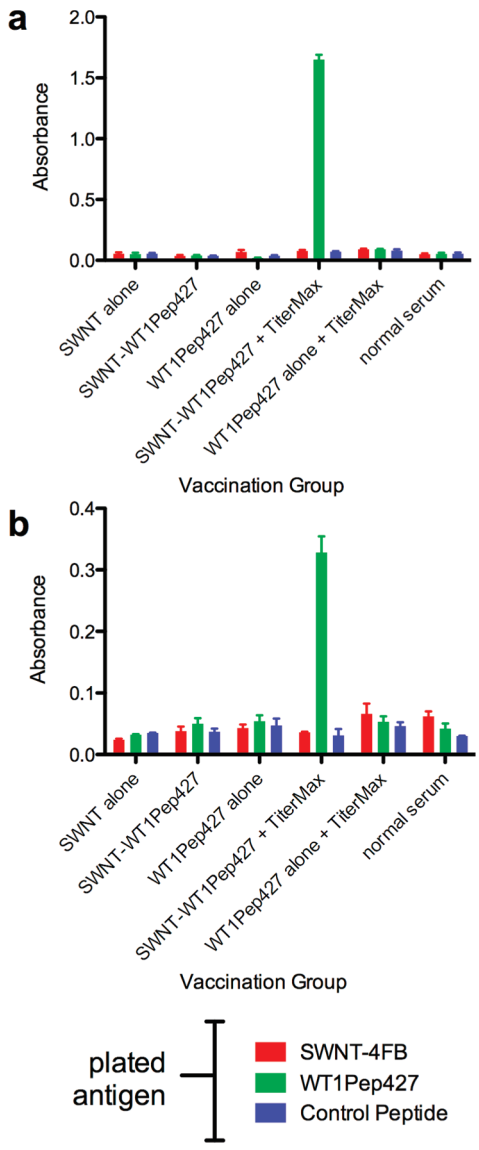

Figure 7. Serum IgG response is specific to WT1Pep427 peptide. Mice were vaccinated with the indicated constructs for four times and a week after final immunization, sera collected from the mice were tested in an ELISA against the indicated antigens at a (a) 1:200 dilution and (b) 1:2000 dilution. The results represent the mean values in triplicate assay ± SD. The figures show representative data from multiple similar experiments.

scaffold (SWNT−4FB) was a polydisperse mixture containing ~0.4 mmol/g of aldehyde groups. The polydispersity of nanotube length may confer some benefit, as it may offer the potential to direct nanotube delivery to several cellular pathways, inducing a broader diversity of immunologic responses. The peptide attachment to the SWNTs formed a spectrally quantifiable chromophore that correlated well with the starting number of aldehyde groups. This linkage is a chemically robust bis-aryl hydrazone that should be stable in physiologic conditions long enough for internalization and trafficking. By spectrophotometrically quantifying the bond formed between the peptides and SWNTs, the amount of covalently bound peptide is more precisely calculated, and the calculation is unaffected by free peptide. We then used these constructs to investigate interactions between SWNTs and human immature dendritic cells, the primary APC of the human immune system. The SWNT−4FB scaffold was robustly internalized and noncytotoxic to DCs up to 100 μg/mL. The SWNT−4FB and SWNT−WT1Pep427 were rapidly internalized and accumulated by DCs, with an uptake pattern consistent with macropinocytosis and subsequent shuttling to MHC class II compartments. We expected the antigenic peptide to be released from SWNTs and presented by the APCs to induce a peptide-specific IgG response. While human CD4 responses to SWNT−WT1Pep427 were comparable to that achieved with peptide alone *in vitro*, the mouse CD4 response to WT1Pep427 *in vitro*, as measured by IFN-γ production in an ELISPOT assay, was poor regardless of conjugation to SWNTs. These results are consistent with the known poorly immunogenic properties of WT1Pep427 in mouse immune cells. When vaccination studies were performed *in vivo* in mice, however, we observed that despite an apparently weak IFN-γ CD4 response *in vitro*, after four immunizations with SWNT−WT1Pep427 conjugates, there was a significantly increased peptide specific IgG response. These results demonstrated the following: (1) Successful delivery and presentation of the peptide *in vivo* can be achieved by use of SWNTs. This suggests that although the same amount of peptide was injected into the mice, the scaffold function of the SWNT may be to improve antigen uptake and presentation by APCs. The SWNT may offer better trafficking and the delivery of the antigens, such as a tissue depot effect, since normally only a small fraction of the dose gains access to the APCs when drugs or antigens are injected in soluble form. Another possibility is that although WT1Pep427 typically produces Th1-type responses (*i.e.*, IFN-γ producing CD4 cells), conjugation to SWNTs redirects the immune response toward a Th2 response. This would shift the response away from IFN-g producing CD4 cells and more toward IL-4 mediated responses. Although IL-4 responsive T cells were not assessed in these experiments, nanoparticulate vaccines have been known to shift responses from Th1 to Th2 responses with increasing particle sizes,[15] and these responses are being investigated by our group. (2) The adjuvant effect is also necessary for the peptide/SWNTs to induce IgG responses, as the peptide/SWNT construct did not induce a significant IgG response either. This requirement is not surprising, as a variety of adjuvants have been shown to be necessary for eliciting antibody responses. The results also suggest that the SWNTs may not stimulate innate immunity as the classic adjuvants do. (3) Peptide mixed with adjuvant did not induce any antibody response. This indicates that adjuvant alone is not sufficient to help a weak MHC class II peptide to induce

an IgG response. Finally, it is intriguing that the conjugation of the peptide to SWNTs could bypass the use of a traditional carrier protein such as keyhole limpet hemocyanin (KLH). In general, the generation of antibody responses against poorly immunogenic tumor antigens is best achieved by conjugating the peptides to a large carrier protein (like KLH), plus an adjuvant.[37] One explanation for the immune response without a carrier protein is the use of a long peptide that has CD4 epitopes in it.[25,26]

Because no immunologic responses to SWNT−4FB alone were observed, using the SWNTs to deliver a poorly antigenic peptide would thus avoid a nonspecific immune response and enable the generation of a more focused, antigen-specific immune response. Overall, this study demonstrates the potential of SWNTs to deliver poorly immunogenic antigens to the immune system, and therefore they are promising tools to explore ways to improve vaccine therapy against cancers and other weakly immunogenic targets.

METHODS

Peptides and Reagents. The peptides used in this study were synthesized by Genemed Synthesis, Inc. (San Antonio, TX) with more than 70% purity. These include a HLA-DR.B1-binding peptide WT1Pep427 derived from human WT1 (RSDELVRHHNMHQRNMTKL) that was used for immunizing mice. A human JAK-2-derived HLA-DR.B1-binding peptide JAK2-DR (GVCVCGDENILVQEF) and BCR.ABL-derived peptide B3A2 (IVHSATGFKQSSKALQRPVASDFE) were used as irrelevant controls.[35] The peptides were dissolved in DMSO and diluted in saline at 5 mg/mL and stored at −80 °C until use. Human granulocyte-macrophage colony-stimulating factor (GM-CSF), interleukin (IL)-1β, IL-4, IL-6, tumor necrosis factor (TNF)-α, prostglandin E2 (PGE2) were also used. Cell isolation kits for human CD14 and CD4 were purchased from Miltenyi Biotec (Bergisch Gladbach, Germany). Human and mouse interferon (IFN)-γ, and mouse IL-4 ELISPOT kits were purchased from Mabtech (Sweden). The horseradish peroxidase (HRP)-anti-mouse IgG and IgM were purchased from Southern Biotechnology Associate Inc. (Brimingham, AL). Adjuvant Titer Max gold was purchased from Sigma-Aldrich Co (St. Louis, MO).

Functionalization of SWNTs. SWNTs produced *via* the high pressure carbon monoxide method were obtained from Unidym, Inc. (Sunnyvale, CA). The nanotubes were 100−1000 nm in length and 0.8−1.2 nm in diameter, as characterized by the manufacturer. The nanotubes were covalently functionalized on their sidewalls according to previously described techniques.[27] This reaction serves to both solubilize the nanotubes and introduce primary amines (SWNT−NH_2). Further purification was accomplished through the use of a C18 Sep-Pak reverse phase cartridge (Waters, Milford, MA), with hydrophilic impurities removed from the relatively hydrophobic SWNTs by washing with 20−25% acetonitrile in 0.1 M tetraethyl ammonium acetate, pH 7. The product SWNT−NH_2 was eluted from the cartridge with at least 50% acetonitrile. The SWNT−NH_2 solid was lyophilized to a dark brown solid and analyzed by UV−vis spectroscopy using a Spectramax M2 spectrophotometer (Molecular Devices, Sunnyvale, CA), transmission electron microscopy (Philips EM-201, Royal Philips Electronics, Amsterdam, Netherlands), and Raman spectroscopy (inVia microRaman system, Renishaw Plc, Gloucestershire, United Kingdom). Amine content was assayed by a quantitative Kaiser ninhydrin assay (Fluka).

Modification of SWNT−NH_2 with Succinimidyl 4-Formyl Benzaldehyde. The purified SWNT−NH_2 in 50% acetonitrile/water was diluted into a reaction buffer of 0.1 M phosphate, 0.15 M NaCl, pH 8 to 20% acetonitrile, and 3−5 g/L of SWNT in the final reaction mixture. To the reaction was added a 10- to 20-fold excess (per amine) of succinimidyl 4-formyl benzaldehyde (Thermo Scientific) dissolved in DMSO. The reaction was allowed to proceed for 2 h after which the pH was raised to 9−10 to quench remaining free linker. The quenched reaction was then purified on a C18 reverse phase cartridge as previously described. The remaining amines on the SWNT−4FB solid were quantified by a Kasier ninhydrin assay,[36] which demonstrated that >95% of amines were capped with benzaldehyde groups. The incorporated benzaldehyde groups were quantified spectrophotometrically by reaction with 0.5 mM 2-hydrazinopyridine. This reaction forms a spectrophotometrically quantifiable bis-aryl hydrazone bond (λ_{max} = 350 nm, ε = 18 000). This reaction was referenced against the reaction buffer alone and the inherent absorbance of the SWNT−NH_2 at 350 nm.

Modification of WT1Pep427 with Hydrazine Linker. The WT1Pep427 peptide was reconstituted in a reaction buffer of 0.1 M phosphate, 0.15 M NaCl, pH 7.5. To the peptide was added a 2-fold excess of succinimidyl hydrazine nicotinamide (Pierce). After 3 h, the peptide was purified from excess linker by size exclusion chromatography on an 1800 Da molecular weight cutoff polyacrylamide gel column (D-Salt, Thermo Scientific) into a 0.1 M MES, 0.15 M NaCl, pH 5.6 buffer. The elution profile was tracked through absorbance at 280 nm, and the purity of the peptide was confirmed by HPLC. The incorporated hydrazine was assayed by reaction of an aliquot of the purfied WT1Pep427-HyNic with 0.5 mM 4FB-PEG (Solulink). This reaction forms a spectrophotometrically quantifiable bis-aryl hydrzone bond (λ_{max} = 354, ε = 29 000). The remaining free amines were quantified through the quantitative Kaiser ninhydrin assay.

Conjugation of SWNT−4FB and WT1Pep427-HyNic. The purified SWNT−4FB and WT1Pep427-HyNic were reacted in a buffer of 0.1 M MES, 0.15 M NaCl, pH 5.5 with 20% acetonitrile in the reaction mixture. Typically, the SWNT concentration was at 0.5−1 g/L, and the peptide was added at a ratio of 0.5−1 mmol of peptide per gram of SWNTs. The reaction mixture was then purified through a C18 cartridge (Waters), with free peptide removed by washing with 20% acetonitrile in 0.1 M TEAA. The pure SWNT−WT1Pep427 conjugate was eluted with 50% acetonitrile in water. The conjugate was lyophilized to a dark brown solid which was then reconstituted with DMSO (99.8%+ biotech grade, Sigma) prior to use in biological assays and vaccinations. SWNT−WT1Pep427 was typically dissolved in DMSO, diluted into PBS, and the final concentration of DMSO in all assay media and injection formulations was less than 0.15% and vehicle controls contained identical amounts of DMSO. For SWNT−WT1Pep427(FITC) conjugates, a custom synthesized peptide was ordered from Solulink, Inc. (San Diego, CA) containing a N-terminal hydrazino nicotinamide and a fluorescein on the lysine side chain of the peptide, and a similar conjugation reaction was performed.

Fluorescent Labeling of SWNT. The purified SWNT−NH_2 material was reconstituted in a reaction buffer of 0.1 M phosphate, 0.15 M NaCl, pH 8 containing 20% acetonitrile to keep the SWNTs from aggregating. To the SWNTs was added the amine reactive succinimdyl ester of Alexa Fluor 555 (Invitrogen), or an equimolar mixture of an amine reactive benzaldehyde terminated linker (PEG4/PFB, SoluLink) and a succinimidyl ester derivative of Alexa Fluor 568 (Invitrogen), at a molar excess of dye/linker to amine. SWNT−WT1Pep427(FITC) conjugates were similarly labeled with a succinimidyl ester of HiLyte Fluor 647 (Anaspec, Inc.). The resulting products were purified on a 10-DG silica gel benchtop size exclusion column into phosphate buffered saline. Dye loading was similar for both the amine (SWNT−NH_2−AF555) and aldehyde (SWNT−4FB−AF568) functionalized materials,

with a range of 0.03−0.1 mmol of dye per gram of SWNTs, calculated spectrophotometrically.

High Performance Liquid Chromatogrpahy (HPLC). All chromatographic analyses were performed on a Beckman Coulter System Gold HPLC system equipped with inline diode array spectral analysis and fluorescence detectors. Data were exported and analyzed using Prism software (GraphPad). All columns were Gemini C18 (Phenomenex). Solvent A was HPLC grade 0.1 M tetra ethyl ammonium acetate (TEAA), and solvent B was 100% acetonitrile. Elution gradients were either 0 to 100% B over 30 min, or 20% B for 10 min followed by a 20 to 100% gradient over 30 min.

Live Cell Microscopy. Immature (day 5) dendritic cells were seeded into 3.5 cm Mattek tissue culture dishes with coverglass bottoms. The cells were supplemented with 5% autologous plasma. Cells were imaged on a Zeiss confocal microscopy system equipped with a temperature-controlled stage. Imaging parameters were verified against control untreated cell samples to rule out autofluorescence. The labeled constructs (in PBS) were added to the DCs at 1−10 μg/mL, in 1−2 mL total volume. Cells were imaged either immediately after the addition of labeled constructs, or after washing with culture medium. Nuclei in live cells were stained with Hoechst 33342 (Invitrogen). Lysosomes were imaged with Lysotracker dye (Invitrogen), and clathrin mediated cytosis was imaged with Texas Red labeled transferrin (Invitrogen) per the manufacturer suggested protocols.

Animals and Immunizations. Healthy female Balb/c mice (6−8 weeks old; Taconic) were housed in the Memorial Sloan-Kettering Cancer Center animal facility. Animals were cared for under institutionally approved animal care and use protocols. The mice were each vaccinated subcutaneously with 20 μg WT1Pep427 peptide, or the peptide conjugated to SWNTs in PBS mixed with an equal volume of TiterMax. SWNTs were suspended in PBS by dissolving solid SWNT−4FB of SWNT−WT1Pep427 in minimal DMSO with subsequent dilution into PBS. Identical procedures and amounts of DMSO were used for vaccination with either peptides, nanotube-peptide conjugates, or nanotubes alone. The amount of SWNTs alone or peptide alone for vaccination was always adjusted to equal nanotube mass in the peptide/SWNT conjugates. Animals were vaccinated with 20 μg peptide per vaccination. For nanotube−peptide conjugates where SWNTs contained 0.4 mmol/g of peptide, 20 μg of peptide correlated with ∼20 μg of SWNT mass. Vaccinations were performed three to four times every two to three weeks and mice were sacrificed for analyses one week after final vaccination.

Enzyme-Linked Immunosorbent Assay (ELISA) for Antibody Detection. Maxisorp plates (96-well) (Nunc, Naperville, IL) were coated with 1 μg of antigen per well in 50 μL of PBS overnight at 4 °C. The wells were blocked with 300 μL of 2% BSA in PBS for 2 h at 37 °C. The plates were washed six times in PBS, and 100 μL of mouse serum diluted in 2% BSA/PBS was added to triplicate wells for 2 h. After the cells were washed, secondary mAbs of antimouse IgG or IgM conjugated to horseradish peroxidase (HRP) was added, and the Ab responses were detected by TMB substrate (Owings Mill, MD), followed by a stop solution of 1 M H_2SO_4. The plates were read at 450 nm wavelength in an Spectramax M2 (Molecular Devices) plate reader. KLH and a standard polyclonal mouse anti-KLH serum were used as a positive control for each experiment. To test antigen binding to wells, identical ELISA assays were also performed with more hydrophobic Polysorp plates with very similar results. The amount of SWNT adsorbed to the plate could not be directly calculated, however.

Generation of Human Monocyte-Derived Dendritic Cells (DCs). After informed consent on Memorial Sloan−Kettering Cancer Center Institutional Review Board approved protocols, peripheral blood mononuclear cells (PBMC) from healthy donors were obtained by Ficoll density centrifugation. CD14+ monocytes were isolated by positive selection using mAb to human CD14 coupled with magnetic beads (Miltenyi Biotec). DCs were generated from CD14+ cells, by culturing the cells in RPMI 1640 medium supplemented with 1% autologous plasma (AP), 500 units/mL recombinant IL-4, and 1000 units/mL GM-CSF. On days 2 and 4 of incubation, fresh medium with IL-4 and GM-CSF was either added or replaced half of the culture medium. For SWNT uptake experiments and microscopy, immature DCs (day 5) were seeded into multiwell tissue culture plates or coverglass bottom microscopy dishes (Mattek) and assayed as described. Alamar blue, ATP lite, and bisbenzimide assays (Invitrogen) were performed as described by the manufacturer.

Isolation and *In Vitro* Stimulation of CD4 T-Cells. The CD4+ T cell fraction from human PBMC was isolated by positive selection using mAbs to human CD4 coupled with magnetic beads (Miltenyi Biotec). For human *in vitro* studies, T cells were stimulated with CD14+ cells as APC (T cells: APC ratio: 10:1), in the presence of 10 μg/mL peptide, SWNTs, or the peptide/SWNT conjugates, and 10 ng/mL IL-15 in the RPMI 1640 supplemented with 5% AP. A week later, the same stimulation protocol was performed using autologous DCs as APCs at a T cell/APC ratio of 30:1. A week after secondary stimulation, the peptide-specific CD4 T cell response was examined by IFN-γ enzyme-linked immunospot (ELISPOT) assay.

IFN-γ ELISPOT. For human studies, HA-Multiscreen plates (Millipore) were coated with 100 μL of mouse antihuman IFN-γ antibody (10 Ag/mL; clone 1-D1K; Mabtech) in PBS, incubated overnight at 4 C, washed with PBS to remove unbound antibody, and blocked with RPMI 1640/10% AP for 2 h at 37 °C. CD4 + T cells were plated with autologous CD14+ APCs (10:1 E/APC ratio), and various test peptides, SWNTs, or conjugates were added to the wells at 20 μg/mL. Negative control wells contained APCs and T cells without peptides or APCs and T cells with irrelevant peptides JAK2-DR. Phytohemagglutinin (PHA, Sigma) at a concentration of 10 μg/mL was used as a positive control for the assay. Microtiter plates were incubated for 20 h at 37 °C and then extensively washed with PBS/0.05% Tween and 100 μL/well biotinylated detection antibody against human IFN-γ (2 μg/mL; clone 7-B6-1; Mabtech) was added. Plates were incubated for an additional 2 h at 37 °C, and spot development was done as described in ref . Spot numbers were automatically determined with the use of a computer-assisted video image analyzer with KS ELISPOT 4.0 software (Carl Zeiss Vision). Data were plotted and interpreted using Prism (GraphPad) data analyses software.

Acknowledgment. Special thanks to the laboratory of Dr. N. Bhardwaj at New York University School of Medicine for providing the human dendritic cells used for microscopy studies. This work was supported by NIH P01 Ca 23766 and Ca33049, NIH R01 Ca55349, The Experimental Therapeutics Center, and The Tudor and Glades foundations.

Supporting Information Available: Additional figures as described in the text. This material is available free of charge *via* the Internet at http://pubs.acs.org.

REFERENCES AND NOTES

1. Graziano, D. F.; Finn, O. J. Tumor Antigens and Tumor Antigen Discovery. *Cancer Treat. Res.* **2005**, *123*, 89–111.
2. Farkas, A. M.; Finn, O. J. Vaccines Based on Abnormal Self-Antigens as Tumor-Associated Antigens: Immune Regulation. *Semin. Immunol.* **2010**, *22*, 125–131.
3. Steinman, R. M.; Banchereau, J. Taking Dendritic Cells into Medicine. *Nature* **2007**, *449*, 419–426.
4. Melief, C. J. Cancer Immunotherapy by Dendritic Cells. *Immunity* **2008**, *29*, 372–383.
5. Dyall, R.; Bowne, W. B.; Weber, L. W.; LeMaoult, J.; Szabo, P.; Moroi, Y.; Piskun, G.; Lewis, J. J.; Houghton, A. N.; Nikolic-Zugic, J. Heteroclitic Immunization Induces Tumor Immunity. *J. Exp. Med.* **1998**, *188*, 1553–1561.
6. Houghton, A. N.; Guevara-Patino, J. A. Immune Recognition of Self in Immunity Against Cancer. *J. Clin. Invest.* **2004**, *114*, 468–471.
7. Heath, A. W. Cytokines as Immunological Adjuvants. *Pharm. Biotechnol.* **1995**, *6*, 645–658.
8. O'Hagan, D. T.; MacKichan, M. L.; Singh, M. Recent Developments in Adjuvants for Vaccines against Infectious Diseases. *Biomol. Eng.* **2001**, *18*, 69–85.

9. Srivastava, P. K.; Menoret, A.; Basu, S.; Binder, R. J.; McQuade, K. L. Heat Shock Proteins Come of Age: Primitive Functions Acquire New Roles in an Adaptive World. *Immunity* **1998**, *8*, 657–665.
10. Kojima, C. Design of Stimuli-Responsive Dendrimers. *Expert Opin. Drug Delivery* **2010**, *7*, 307–319.
11. Livingston, P. O.; Ragupathi, G. Cancer Vaccines Targeting Carbohydrate Antigens. *Hum. Vaccines* **2006**, *2*, 137–143.
12. Reina-San-Martin, B.; Cosson, A.; Minoprio, P. Lymphocyte Polyclonal Activation: A Pitfall for Vaccine Design Against Infectious Agents. *Parasitol Today* **2000**, *16*, 62–67.
13. Xiang, S. D.; Scalzo-Inguanti, K.; Minigo, G.; Park, A.; Hardy, C. L.; Plebanski, M. Promising Particle-Based Vaccines in Cancer Therapy. *Expert Rev. Vaccines* **2008**, *7*, 1103–1119.
14. Fifis, T.; Gamvrellis, A.; Crimeen-Irwin, B.; Pietersz, G. A.; Li, J.; Mottram, P. L.; McKenzie, I. F. C.; Plebanski, M. Size-Dependent Immunogenicity: Therapeutic and Protective Properties of Nanovaccines against Tumors. *J. Immunol.* **2004**, *173*, 3148–3154.
15. Mottram, P. L.; Leong, D.; Crimeen-Irwin, B.; Gloster, S.; Xiang, S. D.; Meanger, J.; Ghildyal, R.; Vardaxis, N.; Plebanski, M. Type 1 and 2 Immunity Following Vaccination Is Influenced by Nanoparticle Size: Formulation of a Model Vaccine for Respiratory Syncytial Virus. *Mol. Pharm.* **2007**, *4*, 73–84.
16. Kostarelos, K.; Bianco, A.; Prato, M. Promises, Facts and Challenges for Carbon Nanotubes in Imaging and Therapeutics. *Nat. Nanotechnol.* **2009**, *4*, 627–633.
17. Kostarelos, K.; Lacerda, L.; Pastorin, G.; Wu, W.; WieckowskiSebastien; Luangsivilay, J.; Godefroy, S.; Pantarotto, D.; Briand, J.-P.; Muller, S.; *et al.* Cellular Uptake of Functionalized Carbon Nanotubes Is Independent of Functional Group and Cell Type. *Nat. Nanotechnol.* **2007**, *2*, 108–113.
18. Kam, N.; O'Connell, M.; Wisdom, J.; Dai, H. Carbon Nanotubes as Multifunctional Biological Transporters and Near-Infrared Agents for Selective Cancer Cell Destruction. *Proc. Natl. Acad. Sci. U.S.A.* **2005**, *102*, 11600–11605.
19. Konduru, N. V.; Tyurina, Y. Y.; Feng, W.; Basova, L. V.; Belikova, N. A.; Bayir, H.; Clark, K.; Rubin, M.; Stolz, D.; Vallhov, H.; *et al.* Phosphatidylserine Targets Single-Walled Carbon Nanotubes to Professional Phagocytes *In Vitro* and *In Vivo*. *PLoS ONE* **2009**, *4*, e4398.
20. Dumortier, H.; Lacotte, S.; Pastorin, G.; Marega, R.; Wu, W.; Bonifazi, D.; Briand, J.; Prato, M.; Muller, S.; Bianco, A. Functionalized Carbon Nanotubes Are Noncytotoxic and Preserve the Functionality of Primary Immune Cells. *Nano Lett* **2006**, *6*, 1522–1528.
21. Mutlu, G. k. M.; Budinger, G. R. S.; Green, A. A.; Urich, D.; Soberanes, S.; Chiarella, S. E.; Alheid, G. F.; Mccrimmon, D. R.; Szleifer, I.; Hersam, M. C. Biocompatible Nanoscale Dispersion of Single-Walled Carbon Nanotubes Minimizes *In Vivo* Pulmonary Toxicity. *Nano Lett.* **2010**, *10*, 1664–1670.
22. Pantarotto, D.; Partidos, C. D.; Hoebeke, J.; Brown, F.; Kramer, E.; Briand, J.-P.; Muller, S.; Prato, M.; Bianco, A. Immunization with Peptide-Functionalized Carbon Nanotubes Enhances Virus-Specific Neutralizing Antibody Responses. *Chem. Biol.* **2003**, *10*, 961–966.
23. Kostarelos, K.; Bianco, A.; Prato, M. Complement Monitoring of Carbon Nanotubes. *Nat. Nanotechnol.* **2010**, *5*, 382–383.
24. May, R. J.; Dao, T.; Pinilla-Ibarz, J.; Korontsvit, T.; Zakhaleva, V.; Zhang, R. H.; Maslak, P.; Scheinberg, D. A. Peptide Epitopes from the Wilms' Tumor 1 Oncoprotein Stimulate Cd4+ And Cd8+ T Cells that Recognize and Kill Human Malignant Mesothelioma Tumor Cells. *Clin. Cancer Res.* **2007**, *13*, 4547–4555.
25. Maslak, P. G.; Dao, T.; Krug, L. M.; Chanel, S.; Korontsvit, T.; Zakhaleva, V.; Zhang, R.; Wolchok, J. D.; Yuan, J.; Pinilla-Ibarz, J.; *et al.* Vaccination with synthetic analog peptides derived from WT1 Oncoprotein Induces T-Cell Responses in patients with complete remission from acute myeloid leukemia. *Blood* **2010**, *116*, 171–179.
26. Krug, L. M.; Dao, T.; Brown, A. B.; Maslak, P.; Travis, W.; Bekele, S.; Korontsvit, T.; Zakhaleva, V.; Wolchok, J.; Yuan, J.; *et al.* WT1 Peptide Vaccinations Induce Cd4 and Cd8 T Cell Immune Responses in Patients with Mesothelioma and Nonsmall Cell Lung Cancer. *Cancer Immunol. Immunother.* **2010**, *59*, 1467–1479.
27. Georgakilas, V.; Tagmatarchis, N.; Pantarotto, D.; Bianco, A.; Briand, J.; Prato, M. Amino Acid Functionalisation of Water Soluble Carbon Nanotubes. *Chem. Commun. (Cambridge)* **2002**, *24*, 3050–3051.
28. Ruggiero, A.; Villa, C. H.; Bander, E.; Rey, D. A.; Bergkvist, M.; Batt, C. A.; Manova-Todorova, K.; Deen, W. M.; Scheinberg, D. A.; Mcdevitt, M. R. Paradoxical Glomerular Filtration of Carbon Nanotubes. *Proc. Natl. Acad. Sci. U.S.A.* **2010**, *107*, 12369–12374.
29. Lacerda, L.; Pastorin, G.; Gathercole, D.; Buddle, J.; Prato, M.; Bianco, A.; Kostarelos, K. Intracellular Trafficking of Carbon Nanotubes by Confocal Laser Scanning Microscopy. *Adv. Mater.* **2007**, *19*, 1480–1484.
30. Sallusto, F.; Cella, M.; Danieli, C.; Lanzavecchia, A. Dendritic Cells Use Macropinocytosis and the Mannose Receptor To Concentrate Macromolecules in the Major Histocompatibility Complex Class II Compartment: Downregulation by Cytokines and Bacterial Products. *J. Exp. Med.* **1995**, *182*, 389–400.
31. Steinman, R. M.; Swanson, J. The Endocytic Activity of Dendritic Cells. *J. Exp. Med.* **1995**, *182*, 283–288.
32. Hewlett, L. J.; Prescott, A. R.; Watts, C. The Coated Pit and Macropinocytic Pathways Serve Distinct Endosome Populations. *J. Cell Biol.* **1994**, *124*, 689–703.
33. Pierre, P.; Turley, S. J.; Gatti, E.; Hull, M.; Meltzer, J.; Mirza, A.; Inaba, K.; Steinman, R. M.; Mellman, I. Developmental Regulation of MHC Class II Transport in Mouse Dendritic Cells. *Nature* **1997**, *388*, 787–792.
34. Watts, C.; Amigorena, S. Antigen Traffic Pathways in Dendritic Cells. *Traffic* **2000**, *1*, 312–7.
35. Maslak, P. G.; Dao, T.; Gomez, M.; Chanel, S.; Packin, J.; Korontsvit, T.; Zakhaleva, V.; Pinilla-Ibarz, J.; Berman, E.; Scheinberg, D. A. A Pilot Vaccination Trial of Synthetic Analog Peptides Derived from the BCR-ABL Breakpoints in CML Patients with Minimal Disease. *Leukemia* **2008**, *22*, 1613–1616.
36. Kaiser, E.; Colescott, R. L.; Bossinger, C. D.; Cook, P. I. Color Test for Detection of Free Terminal Amino Groups in the Solid-Phase Synthesis of Peptides. *Anal. Biochem.* **1970**, *34*, 595–598.
37. Ragupathi, G.; Gathuru, J.; Livingston, P. Antibody Inducing Polyvalent Cancer Vaccine. *Cancer Treat Res* **2005**, *123*, 157–180.